Research

Explanation of High Solar Cell Diode Factors by Nonuniform Contact Resistance

A. S. H. van der Heide[*,†], A. Schönecker, J. H. Bultman and W. C. Sinke
Energy research Centre of the Netherlands ECN, 1755 LE Petten, The Netherlands

*The current density–voltage (**J–V**) curve that characterises the performance of a solar cell is often extra rounded, resulting in reduced efficiency. When fitting to the standard one-dimensional models, it is often found that the rounding cannot be fitted by the series resistance only. In these cases, the diode factor **m** or the depletion region saturation current density $\mathbf{J_{0DR}}$ (depending on the model used) is increased. This behaviour could not be explained so far; this paper discusses if a nonuniform contact resistance of the front side metallisation leads to an increase of m or $\mathbf{J_{0DR}}$.*

*The theoretical part of the investigation is the simulation of the curve for a cell with two regions with different contact resistance. It was found indeed that **m** or $\mathbf{J_{0DR}}$ is increased, while the series resistance is not increased as much as expected.*

*The experimental part was the calculation of the **J–V** curve of a high-**m** solar cell with local contact resistances measured with the so-called Corescan and the cell's resistanceless **J–V** curve as measured with the so-called Suns-$\mathbf{V_{oc}}$ method. The calculated curve approximated the actual curve quite well, demonstrating in practice that high diode factors can be explained by nonuniform contact resistance. Copyright © 2004 John Wiley & Sons, Ltd.*

INTRODUCTION

For an optimum solar cell efficiency, the current density–voltage curve of the illuminated cell must be as rectangular as possible. Although it is known that the curve can be rounded by series resistance, in practice curve shapes are often found that cannot be explained by the single series resistance in the standard one-dimensional models. When fitting such curves by the one-diode model, the diode factor is found to be strongly increased, sometimes to values that are too large to be explained by recombination theory. Several researchers have investigated the influence of two-dimensional parameters on the diode factor and/or the current density–voltage curve. These were emitter sheet resistance,[1–3] in some papers combined with the finger and busbar resistance,[4–7] and a nonuniform minority-carrier diffusion length.[8–13] However, with these parameters only small increases in the diode factor could be explained. The hypothesis tested in this paper is that a

---

* Correspondence to: A. S. H. van der Heide, Energy Research Centre of the Netherlands, Westerduinweg 3, 1755 LE Petten, The Netherlands.
† E-mail: vanderheide@ecn.nl

nonuniform contact resistance of the front side metallisation leads to a high diode factor (which does not mean that there cannot be other reasons for a high diode factor).

First, the electrical characterisation of solar cells and the role of the diode factor will be discussed. After that, the concept of contact resistance and its importance for solar cells will be explained.

The investigation itself is subdivided into a theoretical part and an experimental part. In the theoretical part, the influence of nonuniform contact resistance is simulated for a hypothetical cell that has a part with good contact and a part with bad contact. In the experimental part, the contact resistance is mapped on a cell with a large diode factor with the recently developed and patented[14] Corescan method.[15,16] The contact resistance data are subsequently used in a model to investigate if they can explain the large diode factor of this cell.

Finally, conclusions are drawn and recommendations for appropriate electrical characterisation of solar cells are given.

CHARACTERISING AND ANALYSING SOLAR CELL PERFORMANCE

Solar cell performance indicators

The electrical performance of a solar cell is described by the relation between the current density J flowing through the cell and the potential V across it, while the cell is illuminated. A convenient way to characterise the electrical performance of a solar cell is to specify its open circuit voltage V_{oc}, its short-circuit current density J_{sc} and its fill factor FF. The latter is a measure of the rectangularity of the J–V curve and is defined by:

$$\text{FF} \equiv \frac{V_{mpp} J_{mpp}}{V_{oc} J_{sc}} \tag{1}$$

where V_{mpp} is V at the maximum power point, J_{mpp} is J at the maximum power point and $V_{mpp} J_{mpp}$ is the maximum power per unit of area P_{max}. The graphical interpretation of P_{max} is the area of the largest rectangle below the J–V curve; $V_{oc} J_{sc}$ is the area if the curve were a true rectangle. From the FF definition, it follows that $P_{max} = \text{FF} V_{oc} J_{sc}$. 'The' efficiency of a solar cell η is in fact the efficiency at maximum power delivery, so that $\eta = P_{max}/P_{light}$, where P_{light} is the intensity of the light. It is clear that any loss in FF will reduce the efficiency of the solar cell. Note that V_{oc}, J_{sc} and FF are not fit parameters and do not depend on any model describing the solar cell.

Modeling the currents in a solar cell without resistance influence

The mechanisms governing the solar cell J–V curve depend on the solar cell material; in the following discussion, it is assumed that the cell is made of (multi-)crystalline silicon, as used for 90% of today's production. This cell is in fact a large area p–n diode, and $J(V)$ is given by a term describing J in a dark diode, added with an (oppositely directed) light-generated current density J_L. In the simplest approach, the diode current density J_{NR} is assumed to be due only to recombination of electrons and holes in the neutral regions outside the depletion region, and the influence of resistances is neglected. Then, $J(V)$ is given by:

$$J(V) = J_L - J_{NR} = J_L - J_{0NR}\left(\exp\left(\frac{V}{V_T}\right) - 1\right) \tag{2}$$

where J_{0NR} is the saturation current density of J_{NR} and V_T the thermal voltage, defined by $V_T \equiv kT/q$; k is the Boltzmann constant, T the absolute temperature and q the elementary charge.

To describe the J–V curve of a solar cell more precisely,[17] it is necessary to add a current density J_{DR} for the recombination in the depletion region to Equation (2). Like J_{NR}, J_{DR} is also a diode term, depending

exponentially on V, but in this case the exponent also includes a diode factor for the depletion region m_{DR}. Adding J_{DR} to Equation (2), $J(V)$ according to the so-called two diode model is given by:

$$J(V) = J_L - J_{0NR}\left(\exp\left(\frac{V}{V_T}\right) - 1\right) - J_{0DR}\left(\exp\left(\frac{V}{m_{DR}V_T}\right) - 1\right) \tag{3}$$

where J_{0DR} is the saturation current density of J_{DR}.

In the simplest case, m_{DR} is fixed at 2, independent of V. Although this is not very precise, it is still widely used when fitting J–V curves to Equation (3). An excellent discussion of m_{DR} as a function of V and the junction properties has been given by McIntosh *et al.*[18] Although m_{DR} depends on V, it is often sufficient to use a constant m_{DR} value, being the average value of m_{DR} between 0·2 and 0·4 V, the potential interval where J_{DR} is the most important. Using numerical modelling, McIntosh *et al.* found an average m_{DR} of 1·8 for the highly doped diffused *p*–*n* junctions that are usually applied on solar cells. Note that m_{DR} cannot exceed 2 without extreme assumptions, according to the theory of depletion region recombination.

The other widely used equation for $J(V)$ is related to the more empirical one-diode model. At first sight, there is no need for such an equation since there is the more physical Equation (3). However, it is preferable in situations when it is not possible to determine J_{NR} and J_{DR} correctly. In these cases, using Equation (3) would lead to wrong suggestions about the real problems occuring in the solar cell, as will be shown later on. The one-diode equation is similar to Equation (2), the most important difference being the introduction of the diode factor m in the exponent:

$$J(V) = J_L - J_T = J_L - J_{0T}\left(\exp\left(\frac{V}{mV_T}\right) - 1\right) \tag{4}$$

where J_T is the total recombination current density and J_{0T} the saturation current density of J_T. There is no direct physical interpretation for m, it is used as a fit parameter that determines the roundness of the diode curve. One would expect that $1 < m < 2$, because J_{NR} and J_{DR} that are replaced by J_T have diode factors of 1 and <2, respectively. A low m is preferable, because that results in a more rectangular J–V curve.

Including the influence of resistances on the J–V *curve*

When all resistance losses are neglected, a cell would have an intrinsic fill factor FF_i which depends only on V_{oc} and m and is given to a good approximation by the empirical relation:[19]

$$FF_i = \left[\frac{V_{oc}}{mV_T} - \ln\left(\frac{V_{oc}}{mV_T} + 0\cdot72\right)\right] \bigg/ \left(\frac{V_{oc}}{mV_T} + 1\right) \tag{5}$$

In practice, FF_i will never be reached because series and parallel resistances will always result in a decrease in FF (which can be very large). To give an indication of real FF values, a value of 82·8% was reached for the best laboratory silicon solar cell, while a good value for industrial silicon cells is 76%.

The series and parallel resistance in a cell are usually described by the specific series resistance ρ_{series} and the specific parallel resistance $\rho_{parallel}$. 'Specific' means area independence, obtained by multiplication of the resistance values for the cell with the total cell area. The electrical scheme of the one-diode model including the resistances is shown in Figure 1. By inserting ρ_{series} and $\rho_{parallel}$ in Equation (4), the $J(V)$ relation for the one diode model including resistances is obtained:

$$J(V) = J_L - J_{0T}\left(\exp\left(\frac{(V + J\rho_{series})}{mV_T}\right) - 1\right) - \frac{V + J\rho_{series}}{\rho_{parallel}} \tag{6}$$
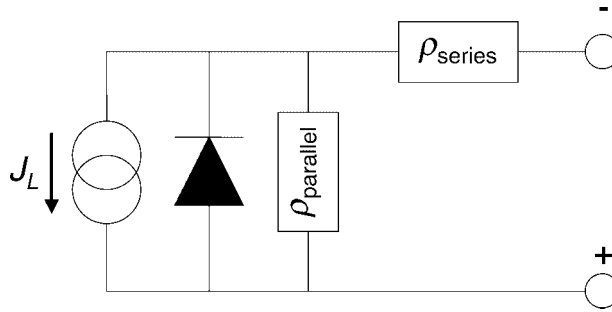
Figure 1. Electrical scheme of the one-diode model of a solar cell, including resistance

For the two-diode model, a similar equation holds. It is standard practice to fit a measured J–V curve to Equation (6) or its two-diode equivalent. To find accurate values for all parameters in Equation (6) is generally difficult because of their strong interdependence in the fit procedure: it is possible to considerably vary several fit parameters with only very little influence on the fit residue.

Increasing ρ_{series} and decreasing $\rho_{parallel}$ both lead to a decrease of the FF; J_{sc} and V_{oc} are almost unaffected unless the resistance problems are really severe.

The different components of the series resistance in a solar cell are the sheet resistance ρ_s of the emitter (*n*-type region), the bulk resistance of the base (*p*-type region), the contact resistance between metallisation and silicon at the front and back surfaces and the resistance of the metallisation itself. Almost all series resistance is due to sources at the front side, because the fraction covered with metal must be minimised on this side. It is clear that, in reality, the series resistance is of distributed nature, while ρ_{series} is a single 'lumped' value. This lumping approach is valid only when potential differences across the cell are small: when they are larger than V_T, owing to large differences in local series resistance, the approach breaks down because the resistance sources can no longer simply be added, because of the nonlinear behaviour of the equations.[20] The fit artefacts that result from strongly varying series resistance were described recently by Bowden and Rohatgi;[21] as origins for local series resistance differences they correctly mentioned high finger resistivity and finger interruptions, but not the possibility of nonuniform contact resistance. However, nonuniform contact resistance should be addressed since it is the most important source of local series resistance differences on many cells.

CONTACT RESISTANCE IN SOLAR CELLS

In general, the relation between the current density J_c through the contact and the potential V_c across it is non-linear for metal–semiconductor contacts. Therefore, the specific contact resistance ρ_c ($\Omega\,\mathrm{cm}^2$) is defined in the following way:[22]

$$\rho_c \equiv \left(\left. \frac{\mathrm{d}J_c}{\mathrm{d}V_c} \right|_{V_c=0} \right)^{-1} \tag{7}$$

It is possible to fabricate contacts with a linear $J_c(V_c)$ relation. For such 'ohmic contacts', the definition reduces to:

$$\rho_c = \frac{V_c}{J_c} \tag{8}$$

Ohmic contacts on silicon are obtained by using a high doping level at the surface. In this way, the thickness and height of the potential barrier at the metal–silicon interface is reduced and tunnelling through the barrier, which depends linearly on V_c, becomes the predominant conduction mechanism.

Different methods have been used to deposit the metal contacts on solar cells. Although metal deposition by evaporation produces the best contacts, this method is used only for high-efficiency laboratory cells because it is too expensive for production. Currently, screen-printing a metal paste followed by sintering is used for the deposition of the metal contacts on almost all industrial crystalline silicon solar cells.

Although the contact between the fingers and the silicon is usually characterised by ρ_c, there are several drawbacks to that approach. In the first place, the metal–silicon interface for screen-printed fingers is known to be nonuniform in structure and composition,[23] so that ρ_c will vary across the finger width. The characterisation by a single 'average' ρ_c value is therefore inappropriate, in particular because the model used to calculate ρ_c assumes a constant ρ_c across the finger width. In the second place, it is not only ρ_c, but also the sheet resistance of the emitter below a finger $\rho_{s,bf}$, that determines the total resistance for the lateral current that flows into a finger. The value of $\rho_{s,bf}$ is generally unknown, but it is typically several times higher than ρ_s because part of the emitter dissolves in the finger during sintering.[24]

Therefore, the best way is to avoid the use of ρ_c and to define a so-called line contact resistance in which the emitter resistance below the finger is included, as has been proposed previously in a more general context by Berger.[25] Here, a slight modification is necessary to make it more appropriate for parallel line contacts such as the fingers on a solar cell. The line contact resistance R_{cl} (Ω cm) is then defined as

$$R_{cl} \equiv \left(\left. \frac{di_c}{dV_{ce}} \right|_{V_{ce}=0} \right)^{-1} \tag{9}$$

where i_c is the total current flowing through the contact area per unit length of line (called 'finger' in the case of a solar cell), and V_{ce} is V_c, the potential across the contact, at the edge of the line/finger (the position must be defined in this case, as V_c varies below a contact that collects lateral currents).

For ohmic contacts, this definition reduces to:

$$R_{cl} = \frac{V_{ce}}{i_c} \tag{10}$$

The units of R_{cl} are Ω cm. A method that enables mapping of R_{cl} on a solar cell is described in the experimental part of this paper.

THE INFLUENCE OF NONUNIFORM R_{CL} IN THEORY

The influence of a nonuniform R_{cl} on a cell's total J–V curve is simulated by averaging two J–V curves, one calculated for the area between two well-contacted fingers and one calculated for the area between two badly contacted fingers.

Calculating the J–V curve for the area between a finger pair

The model used for the calculation of the J–V curve between two fingers is shown in Figure 2. Let J_F be defined as the total current produced between two fingers divided by the total area between these fingers, and let the finger potential be denoted by V_F. To simplify the calculation of the J_F–V_F curve, several assumptions are made. The potential at both fingers is assumed to be equal, R_{cl} is also assumed to be equal for both fingers, the sheet resistance and the local J–V curve are both assumed to be independent of position. The current is assumed to flow vertically in the base and horizontally in the emitter. The current across the junction in the region below the finger is not taken into account in the calculation. It is assumed that the locally generated current density $J(x)$ can be described by Equation (4), where V is substituted by $V(x)$.

The assumptions are reasonable and are used to avoid an unnecessarily complicated model. By their nature, they are not critical for a general assessment of the effect of contact resistance nonuniformity.

As $J(x)$ follows directly from $V(x)$, it is necessary and sufficient to calculate $V(x)$ at each position between the fingers for the calculation of the total current produced between the fingers, and thus J_F as a function of V_F. The differential equation and boundary conditions that determine $V(x)$ will now be derived.
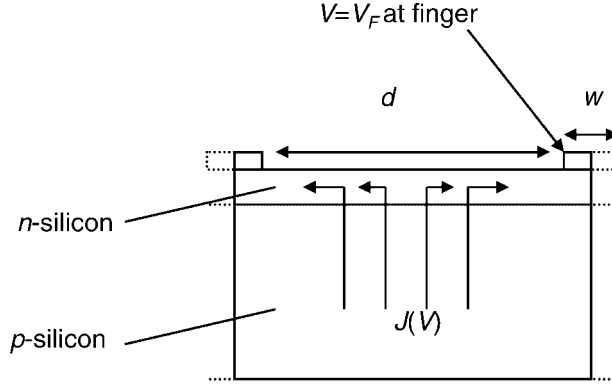
Figure 2. Model used to calculate the current produced between two fingers

Let the current to the finger, per unit length of finger, be denoted by i. The gradient of i is equal to $J(x)$, given by Equation (4):

$$\frac{\mathrm{d}i}{\mathrm{d}x} = J_{\mathrm{L}} - J_{0\mathrm{T}}\left(\exp\left(\frac{qV(x)}{mkT}\right) - 1\right) \tag{11}$$

The emitter is a normal resistive layer, so that i is related to $\mathrm{d}V/\mathrm{d}x$ by:

$$i = -\frac{1}{\rho_{\mathrm{s}}}\frac{\mathrm{d}V}{\mathrm{d}x} \tag{12}$$

Substituting Equation (12) in (11) gives the differential equation:

$$\frac{\mathrm{d}^2V}{\mathrm{d}x^2} = -\rho_{\mathrm{s}}\left[J_{\mathrm{L}} - J_{0\mathrm{T}}\left(\exp\left(\frac{V(x)}{mV_{\mathrm{T}}}\right) - 1\right)\right] \tag{13}$$

The first boundary condition is the one at the position $x = 0$, defined to be the point as close as possible to the edge of a finger:

$$V(0) = V_{\mathrm{F}} + V_{\mathrm{ce}} = V_{\mathrm{F}} + 2\frac{R_{\mathrm{cl}}}{\rho_{\mathrm{s}}}\frac{\mathrm{d}V}{\mathrm{d}x}\bigg|_{x=0} \tag{14}$$

where V_{ce} was calculated by recognising that i_{c} for a finger is $2|i|$, i being given by Equation (12) at the edge of a finger, and substituting this expression in Equation (10). The factor of 2 accounts for the fact that current enters the finger from two directions, the absolute value of i has to be taken because only the magnitude of i is important in this case, not the direction.

The second boundary condition follows from the assumed symmetry in V_{F} and R_{cl}, which makes $V(x)$ symmetrical, so that the maximum potential must be reached at the point exactly between the fingers:

$$\frac{\mathrm{d}V}{\mathrm{d}x}\bigg|_{x=\frac{d}{2}} = 0 \tag{15}$$

where d is the distance between the finger edges.

Equation (13) can only be solved numerically, which was done using the method of finite differences. The solution for $V(x)$ represented as $V(x)$-V_{F} is shown for different values for R_{cl} and V_{F} in Figure 3. The other parameters were fixed at $\rho_{\mathrm{s}} = 50\,\Omega$, $J_{\mathrm{L}} = 30\,\mathrm{mA/cm}^2$, $m = 1{\cdot}3$ and $J_{0\mathrm{T}}$ is chosen so that $V_{\mathrm{oc}} = 580\,\mathrm{mV}$.

When V_{F} or R_{cl} increase, J_{F} decreases, because $V(x)$ is shifted upwards. The current decrease with increase of V_{F} is clearly reflected in the flattening of $V(x)$ in the case of $V_{\mathrm{F}} = 570\,\mathrm{mV}$, as shown in Figure 3. That an increase of R_{cl} causes an additional flattening at a large forward potential is clear from the difference between the 0·5 and
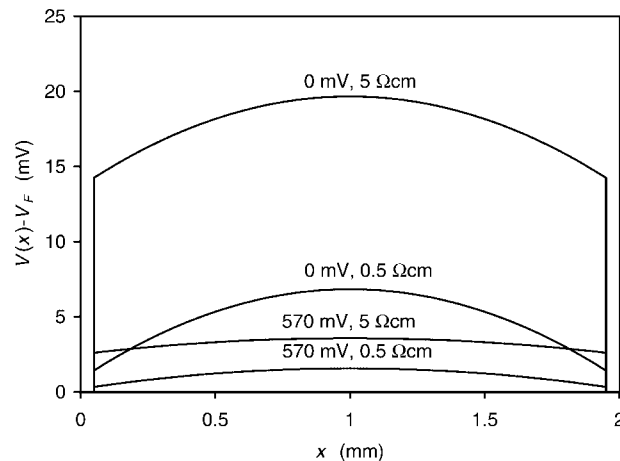
Figure 3. $V(x)-V_F$ between a finger pair calculated for different values of V_F and R_{cl}

$5\,\Omega\,\text{cm}$ curves at $570\,\text{mV}$. The reason is that the $J–V$ curve is already strongly decreasing near $570\,\text{mV}$ and all potentials between the fingers are shifted upwards when the contact resistance at the fingers is higher.

It is important to note that the number of different potentials between the fingers is in fact infinite, so that the exact calculation of the total current would involve the summation of an infinite number of exponentials (this is of course the case for any nonuniform potential). Therefore, it is impossible to fit a $J–V$ curve exactly by one or two exponential terms, as is done by the standard one-dimensional diode models. As mentioned before, a good approximation to the infinite summation of exponentials is the usually applied concept of a lumped series resistance ρ_{series}. However, this approximation is only valid if the potential differences are small compared with V_T.

Calculation of the J–V *curve for a cell with a good and bad contact region and its analyis*

Using the numerical simulation, $J_F–V_F$ curves were calculated for $R_{cl} = 1\,\Omega\,\text{cm}$ ('good') and for $R_{cl} = 15\,\Omega\,\text{cm}$ ('bad'); the value of ρ_s was $50\,\Omega$ in both cases. The averaged $J–V$ curve, representing the curve for a cell with a well-contacted and a badly contacted region, was calculated by summing the J_F values at each V_F and dividing by 2. It was assumed that the one-diode formula (Equation 4) describes the $J–V$ curve for each point between the fingers correctly, where m is $1 \cdot 3$. The three curves were all fitted to the one-diode equation including resistances Equation (6), using two different fit methods, both based on the least-squares method, but with a different weighting of the individual measurement points. The first fit method uses the same weighting for all points (uniform weighting), the other method uses weighting according to the so-called orthogonal distance regression method (ODR).[26] The latter method compensates for the too large influence on the fit result of a small voltage noise at voltages near V_{oc} in the case of uniform weighting. The calculated curves and their fit parameters (for uniform weighting, since that is generally used) are shown in Figure 4.

The fit parameters for the $J_F–V_F$ curves for good and bad contact are as expected: the fitted value for m is equal to the value used for the calculation of the curve, and the fitted value of ρ_{series} is the value expected for the values of R_{cl} and ρ_s that have been used. In contrast, fitting the averaged curve with the usual method of uniform weighting results in a strongly increased m of $2 \cdot 19$ and a ρ_{series} that is only slightly increased. It is clear that the lumped series resistance model fails here, because the potential differences across the hypothetical cell are too large. This example also shows that m can easily reach a value larger than 2. This is important to note because this could not be explained so far, because currents due to recombination have $m < 2$. It should be mentioned that the fit method can have a considerable influence on the fitted values of m and ρ_{series}: in case of fitting with the ODR method, it was found that $m = 1 \cdot 67$ and $\rho_{\text{series}} = 1 \cdot 21$. This result is considerably better in the sense that the local bad contact is better represented in an increased series resistance, but m is still clearly higher than $1 \cdot 3$ and ρ_{series} is still somewhat low.

Performing a two-diode fit with $m_{DR} = 2$ to the averaged curve, the fitted value of J_{0DR} showed a four-fold increase compared with the value for the individual curves, while the value of J_{0N} was decreased to a negligible
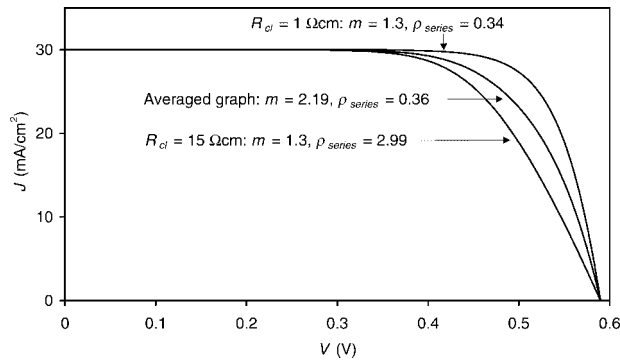
Figure 4. J–V curves for well-contacted fingers and badly contacted fingers and the average curve, the latter being the curve for a hypothetical cell with a well-contacted and a badly contacted region
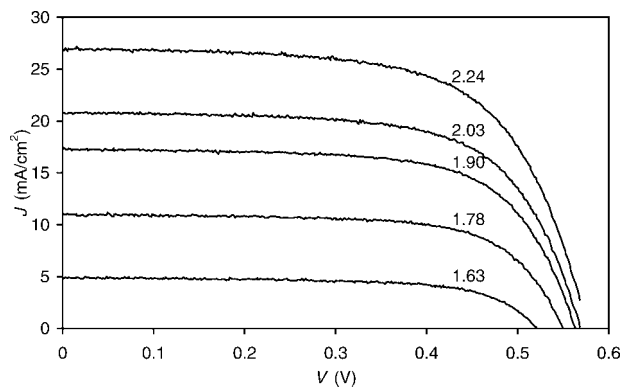

Figure 5. J–V curves for a cell with locally increased contact resistance, measured at different light intensities. The m values found for fitting with uniform weights are indicated

value. It is clear that it is wrong to interpret a high J_{0DR} as a high depletion region recombination rate in case of large R_{cl} differences. To avoid wrong conclusions from the fit parameters for such cells, it would be better to use the empirical one-diode model instead of the two-diode model. It is even questionable if one should try to fit one of the standard one-dimensional equations to such a curve at all, since these models cannot account correctly for large two-dimensional potential differences.

An interesting consequence of the fact that the high m is caused by resistance instead of recombination is that the m value will increase with increasing light intensity, since the potential differences over the cell increase. This is illustrated in Figure 5, where J–V curves for one cell with a locally increased contact resistance are shown for different light intensities. Note that the annual production for a cell with large contact resistance problems will be higher than would be expected from the one sun J–V curve, since FF increases with decreasing light intensity.

THE INFLUENCE OF NONUNIFORM R_{CL} IN PRACTICE

The experimental approach was the following: take a cell with a high m; map the contact resistance on this cell, measure how the J–V curve would have been without any series resistance influence; and calculate if the difference between this curve and the real J–V curve can be explained with the measured contact resistances.

The calculation of the cell J–V curve is performed by the calculation of local J–V curves, using the measured local series resistance data and an assumed local series resistanceless J–V curve, followed by averaging of the local J–V curves. The local series resistanceless J–V curve is assumed to be equal to the curve for the entire cell, that has been determined with the Suns-V_{oc} method.[27]
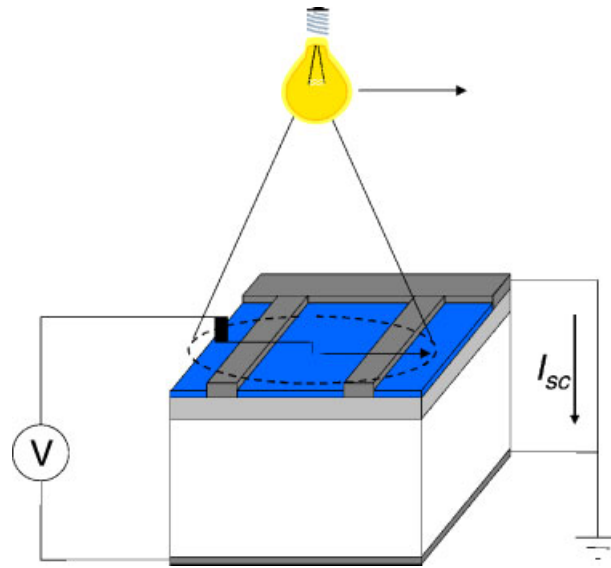
Figure 6. Schematical drawing of the Corescan method

The cell under investigation is a 10×10 cm screen-printed multicrystalline silicon solar cell with $m = 2.41$. The parallel resistance of the cell was high enough to avoid any significant influence on FF, but the large m value was already enough to result in FF 68.3%.

The Corescan method

The instrument used for contact resistance scanning is the Corescan,[15,16] derived from COntact REsistance scan. The instrument is based on the mapping of the potential $V(x,y)$ on an illuminated, short-circuited cell. The patented[14] technique it uses is displayed in Figure 6.

The local illumination of the cell induces current, which induces potential gradients across fingers, busbars and emitter, and potential 'jumps' at the finger edges. The steepness of the gradients and the height of the potential jumps are a measure of the different series resistance sources. The potential jumps are proportional to the contact resistance and the induced current density.

The measurement of a 10×10 cm cell takes 6 min, at a lateral resolution of 0.1 mm perpendicular to the fingers and 2 mm parallel to the fingers. The probe is centred in a uniform light beam with diameter $>2d$, where d is the distance between the fingers. Short-circuiting of the cell by connecting the busbars to the backsurface is used to ensure that $J(x,y)$ is as constant as possible across the cell, which is necessary for an optimum accuracy. The reason is that the J–V curve is practically flat up to 0.35 V, so that $J(x,y) = J_{sc}(x,y) = J_L(x,y)$ for all (x,y). Of course there are variations in $J_L(x,y)$ due to material quality differences, but these are $<10\%$. These differences lead to relative errors of the same magnitude in the series resistance sources calculated from the measurements. Since these errors are small compared with the variations in series resistance sources for low-FF solar cells, $J_L(x,y)$ is simply assumed to be constant by the Corescan instrument. The current density induced by the beam should be kept at or below J_L for one sun illumination, to minimise errors due to possible non-ohmic behaviour of the finger contact at high current densities.

An example of a line scan measured with the Corescan is shown in Figure 7; many of these line scans together are used to create the usual two-dimensional potential maps. The potential jumps at the fingers due to contact resistance can be clearly observed; large differences in contact resistance over a short distance are found on this cell.

The analysis of $V(x)$ between the fingers during a Corescan is simplified because the cell is short-circuited during a Corescan, so that Equation (13) reduces to

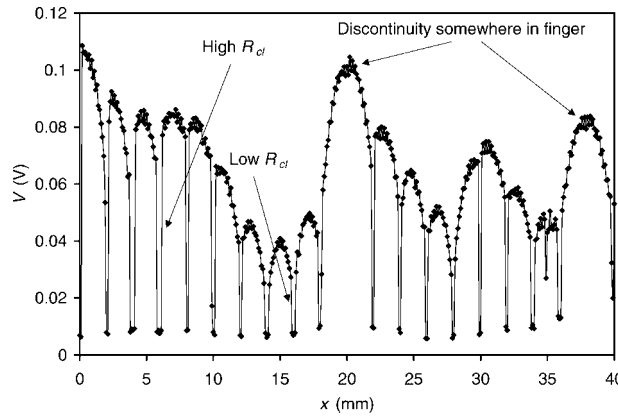$$\frac{\mathrm{d}^2 V}{\mathrm{d}x^2} = -\rho_s J_{\text{Corescan}} \tag{16}$$

Figure 7. Example of one scan line as measured with the Corescan method

where J_{Corescan} is the effective light generated current density at which the Corescan is performed. This current density is lower than the current I_{sc} divided by the beam area A, owing to shadowing of the probe and current flow parallel to the fingers to the dark region outside the beam. An empirical relation is used in practice, $J_{\text{Corescan}} = C(I_{\text{sc}}/A)$, where C is a calibration constant. C is determined by dividing the Corescan potential jumps on a certain cell by the potential jumps observed for the uniform illumination in a solar simulator. For the set-up used, $C = 0.6$ was found.

The differential equation has the general solution of a parabola:

$$V(x) = -\frac{1}{2}\rho_{\text{s}}J_{\text{Corescan}}x^2 + C_1 x + C_2 \tag{17}$$

where C_1 and C_2 are integration constants that are determined by the R_{cl} and V_{F} values at the fingers. These parabolas are easily observed in Figure 7, being symmetrical between fingers with equal R_{cl} and being asymmetrical between fingers with strongly differing R_{cl} values.

Now R_{cl} will be calculated; it was found by experience that even bad contacts on solar cells are still ohmic, so that Equation (10) can be used. This equation contains the parameter i_{c}, which can be approximated by $J_{\text{Corescan}}d$, but this approximation is insufficient when there is a large R_{cl} difference between adjacent fingers. A better value for i_{c} can be obtained from Equation (12), that relates the flow of a lateral current to $\mathrm{d}V/\mathrm{d}x$. The value of $\mathrm{d}V/\mathrm{d}x$ is not necessarily the same on the left and the right edge of a finger, so that the final expression for R_{cl} reads

$$R_{\text{cl}} = \frac{V_{\text{ce}}}{i_{\text{c}}} = \frac{V_{\text{ce}}}{\frac{1}{\rho_{\text{s}}}\left(\left|\frac{\mathrm{d}V}{\mathrm{d}x}(\text{left})\right| + \left|\frac{\mathrm{d}V}{\mathrm{d}x}(\text{right})\right|\right)} \tag{18}$$

where absolute values have been taken because only the magnitude of the current must be used here, the direction information has to be removed.

In principle, also the metallisation resistances can be determined from the measured potentials. However, this is not so accurate since the local illumination makes the method less sensitive for the metallisation resistance. One could say that the effective J for the metallisation is much lower than J_{Corescan} because of the local illumination, since most of the metallisation pattern is in the dark. When one is interested only in R_{cl} and ρ_{s}, it is even an advantage to be insensitive for the metallisation resistance, because there is no position dependent metallisation potential superimposed on the potential due to R_{cl} and ρ_{s}.

In this paper, the Corescan is used to determine a local specific series resistance $\rho_{\text{series}}(x,y)$ from the $V(x,y)$ data measured during the scan. It is defined as:

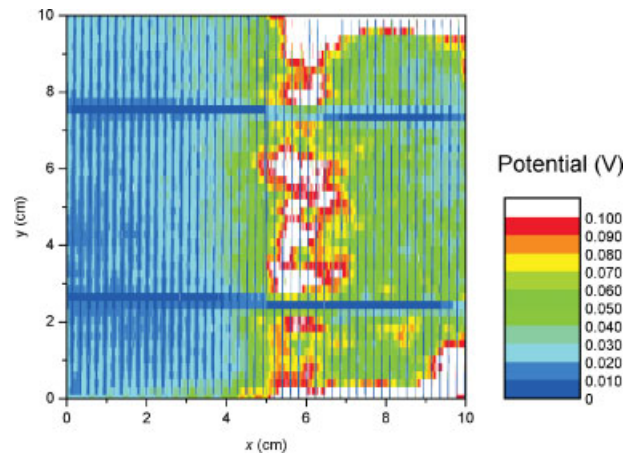$$\rho_{\text{series}}(x,y) \equiv \frac{V(x,y)_{\text{Corescan}}}{J_{\text{Corescan}}} \tag{19}$$

Figure 8. Corescan on the cell with high *m*, on the left and right the contact resistance is low, near the centre it is high. This cell was measured in a left and a right part, this is no longer necessary

In the case of the Corescan the metallisation influence is underestimated and R_{cl} and ρ_s are mainly responsible for $\rho_{series}(x,y)$. This would be a problem when metallisation resistance plays an important role, but the FF of the investigated cell is so low (68·3%) that the metallisation resistance can be neglected in the FF loss. If this assumption is incorrect, it will become apparent because it will not be possible to explain the shape of the measured *J–V* curve from $\rho_{series}(x,y)$.

Corescan on cell with nonuniform R_{cl} and using the data to predict the J–V curve

The Corescan on the investigated cell was performed at $J_{Corescan} = 22$ mA/cm^2 and the resulting $V(x,y)$ distribution is shown in Figure 8. By performing two scans at other light intensities it was found that the contact between fingers and silicon is ohmic everywhere for $J_{Corescan} = 10$–30 mA/cm^2.

High potentials were measured on a large part of the cell, indicating serious series resistance problems in that region. Detailed observation of $V(x,y)$ shows that a high R_{cl} is responsible for the series resistance problems: the maximum potential between the fingers is almost entirely due to the potential jump at the finger, there is no high parabola as would be expected for a very high ρ_s. From the $V(x,y)$ values, $\rho_{series}(x,y)$ values (that are consequently mainly determined by R_{cl}) are calculated from Equation (19) and will be used for the calculation of the *J–V* curve of the entire cell.

From other research into the reasons for bad contact, it is most probable that too low a peak firing temperature in the bad contact region is the reason in this case. The lower temperature in this region is the result of a local reduction of infrared radiation caused by the presence of a quartz belt support in the infrared belt furnace that was used.[28]

In addition to $\rho_{series}(x,y)$, the local series resistanceless *J–V* curves are needed to calculate the *J–V* curve of the complete solar cell. As an approximation, the series resistanceless *J–V* curve of the entire cell is assumed to be valid for all (x,y). This *J–V* curve is constructed using the Suns-V_{oc} method[27] and the first part of the dark *J–V* curve, that has been shifted over J_{sc} at 1 sun. The Suns-V_{oc} method measures V_{oc} during the intensity decay of a flash light; in this way no current flows in the cell and there is no influence of series resistance. The intensity is measured at the same time with a reference cell. Plotting J_L as a function of V_{oc} gives the diode part of the solar cell *J–V* curve; shifting this diode curve over J_{sc} at 1 sun gives the resistanceless *J–V* curve at 1 sun. Of course, this method depends on the assumption that the recombination rates are independent of light intensity.

The Suns-V_{oc} method is not so appropriate for the measurement of the (almost) horizontal first part of the *J–V* curve. Very low intensities have to be used to construct this part, resulting in accuracy problems when determining the correct intensity and V_{oc}. These measurement problems were avoided by using another method for this part of the curve: measurement of the dark *J–V* curve and shifting it upwards over J_{sc} at 1 sun. The idea
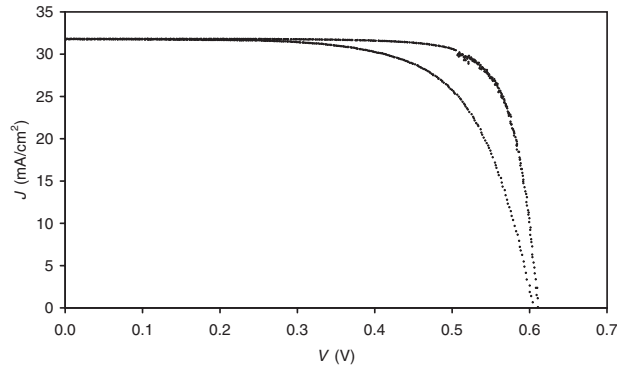
Figure 9. Series resistanceless J–V curve constructed with the Suns-V_{oc} method and dark J–V curve (upper curve) and the real J–V curve. The large difference indicates a large series resistance problem

behind using a shifted dark J–V curve is that series resistance can be neglected in the measurement of the dark J–V curve as the currents are very low, at low voltages at least. By shifting of the curve it is assumed again that recombination rates do not change too much with light intensity, as is a generally accepted practice for crystalline Si solar cells.

The fill factor of the series resistanceless curve will be denoted by FF_{Rs0} in the following. The total series resistanceless J–V curve for the high-m cell is shown, together with the normal curve, in Figure 9. In contrast to the normal curve with $m = 2 \cdot 41$ and $FF = 68 \cdot 3\%$, the values for the series resistanceless curve are $m = 1 \cdot 14$ and $FF_{Rs0} = 79 \cdot 6\%$. This shows that there is much series resistance present in this cell.

The method of obtaining a curve that is not influenced by series resistance also enables another way to quantify series resistance, namely by a parameter ΔFF_{Rs} defined as follows:

$$\Delta FF_{Rs} \equiv FF_{Rs0} - FF \tag{20}$$

This parameter does not depend on fit models, does directly give the series resistance loss and its determination does not depend on the assumption of one-dimensionality. For the most general use, it would be better to determine and specify this value instead of the usual ρ_{series}.

By substitution of the measured $\rho_{series}(x,y)$ for ρ_{series} in Equation (6) and using the series resistanceless J–V curve as the local J–V curve for all (x,y) it is possible to calculate $J(V)$ for all 47850 Corescan points. The average of these curves is the J–V curve of the entire cell. As there are so many points, it is more efficient to divide the $\rho_{series}(x,y)$ data in 50 classes, as shown in Figure 10. In this way, only 50 J–V curves have to be calculated. The total J–V curve is then found by a weighted average of these 50 J–V curves with the number of points in a class as weighting factors. By doing so, the individual points on the cell are assumed to be independent. Of
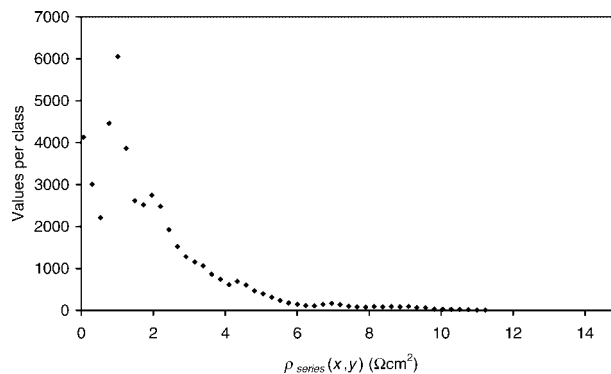

Figure 10. Histogram showing the number of locations for a specific ρ_{series} interval
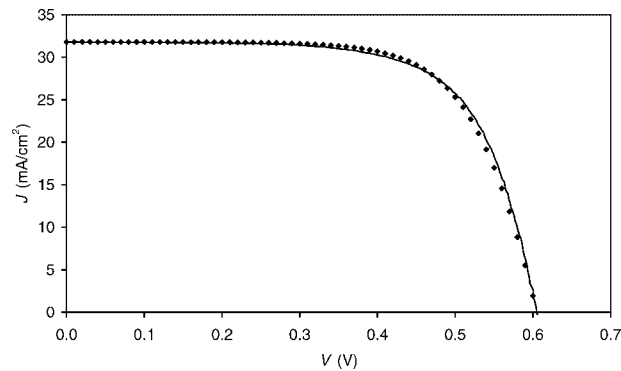
Figure 11. Comparison of predicted J–V curve (individual points) and measured J–V curve (continuous line)

course, this is not fully correct since lateral current flow is possible within a solar cell, but the emitter sheet resistance of around $50\,\Omega$ suppresses long-distance current flows. As an illustration, the maximum potential between two fingers at 1 sun would already increase to $500\,mV$ when they would be separated by $2\,cm$. If these long-range currents would not be suppressed, the Corescan principle would not work at all, since the current generated in a bad contact area could easily flow to a region with good contact so that potential jumps would nowhere be measured. Because the cell currently investigated shows a contact resistance distribution where the good and the bad area is roughly divided in two large parts, lateral current flow from the bad area to the good area can be neglected and the points may be considered independent indeed.

The resulting average J–V curve for the complete cell is shown together with the measured curve in Figure 11. Although the difference between the curves is quite small, m was found to be $1{\cdot}97$ for the calculated curve compared with $2{\cdot}41$ for the measured curve. This difference is caused by the fact that the fit parameters are quite sensitive to small curve differences, as was mentioned earlier. The small differences between calculated and measured curve can be explained by small deviations from the assumptions made. Nevertheless, the shapes of the J–V curves are almost the same and the difference in FF is only $0{\cdot}1\%$, which leads to the conclusion that the difference between the resistanceless J–V curve and the real J–V curve is caused by a high and nonuniform R_{cl} indeed.

CONCLUSIONS

In this paper, it has been demonstrated, by means of theoretical simulations and calculations with actually measured R_{cl} values, that large R_{cl} variations across a cell cause an increase of the diode factor m or a high J_{0DR} instead of a high lumped series resistance. So series resistance and J_{0DR} values fitted from the J–V curve at one sun illumination have no meaning in practice, other means have to be used to determine them. J_{0DR} should be determined from the dark J–V curve, since the disturbing series resistance effects are much smaller for the low currents flowing in the dark. Series resistance should even be specified in another way than by the usual value ρ_{series}, namely by the FF loss due to series resistance ΔFF_{Rs}. This value can be obtained by measuring the series resistanceless FF with the Suns-V_{oc} method, and subtracting the real FF from it.

REFERENCES

1. Chambouleyron I. Solar cell sheet resistance analysis. *Proceedings of the 1st European Photovoltaic Solar Energy Conference*, 1977; 987–995.
2. Bobbio S, Califano FP, Ciccarone E. Non-linear analysis of solar-cells-series resistance. *Proceedings of the 1st European Photovoltaic Solar Energy Conference*, 1977; 1006–1018.

 3. Bouazzi AS, Abaab M, Rezig B. The effect of the emitter resistivity on the characteristics of a silicon solar cell. *Proceedings of the 14th European Photovoltaic Solar Energy Conference*, 1997; 2477–2479.

 4. Calzolari PU, Mazzone AM. Numerical modelling of a solar cell in three dimensions. *Proceedings of the 2nd European Photovoltaic Solar Energy Conference*, 1979; 631–638.

 5. Bell RO. Measurement and analysis of *I–V* curves as applied to EFG solar cells. *Proceedings of the 9th European Photovoltaic Solar Energy Conference*, 1989; 386–389.

 6. Potts A, Parrott JE. Modelling of distributed resistance in solar cell devices. *Proceedings of the 11th European Photovoltaic Solar Energy Conference*, 1992; 306–309.

 7. Maroto JC, Araújo GL. Three-dimensional circuit analysis applied to solar cell modelling. *Proceedings of the 13th European Photovoltaic Solar Energy Conference*, 1995; 1246–1249.

 8. Drope K, Möller HJ. Modeling of the *I–V* characteristics of multicrystalline solar cells with inhomogeneous distribution of electrical parameters. *Proceedings of the 12th European Photovoltaic Solar Energy Conference*, 1994; 1359–1362.

 9. Bell RO. Effect of non-uniformities of diffusion length and local defects on solar cell performance. *Proceedings of the 13th European Photovoltaic Solar Energy Conference*, 1995; 1231–1234.

10. Baldner R, Lautenschlager H, Schetter C, Schindler R, Warta W. Open circuit voltage losses in multicrystalline silicon: an investigation by mini solar cells (MSC). *Proceedings of the 25th IEEE Photovoltaic Specialists Conference*, 1996; 641–644.

11. Gee JM, Sopori BL. The effect of gettering on areal inhomogeneities in large-area multicrystalline-silicon solar cells. *Proceedings of the 26th IEEE Photovoltaic Specialists Conference*, 1997; 155–158.

12. Warta W, Sutter J, Wagner BF, Schindler R. Impact of diffusion length distributions on the performance of mc-silicon solar cells. *Proceedings of the 2nd World Conference on Photovoltaic Energy Conversion*, 1998; 1650–1653.

13. Mijnarends PE, Janssen GJM, Sinke WC. The effect of material inhomogeneities on the characteristics of semicrystalline silicon solar cells: the second diode. *Solar Energy Materials and Solar Cells* 1994; **33**: 345–360.

14. Patent number WO0126163, priority date 4 October 1999.

15. van der Heide ASH, Schönecker A, Wyers GP, Sinke WC. Mapping of contact resistance and locating of shunts on solar cells using Resistance Analysis by Mapping of Potential (RAMP) Techniques. *Proceedings of the 16th European Photovoltaic Solar Energy Conference*, 2000; 1438–1442.

16. van der Heide ASH, Bultman JH, Hoornstra J, Schönecker A. Error diagnosis and optimisation of c-Si solar cell processing using contact resistances determined with the Corescanner. *Solar Energy Materials and Solar Cells* 2002; **74**(1–4): 43–50.

17. Sah CT, Noyce RN, Shockley W. Carrier generation and recombination in *p-n* junctions and *p-n* junction characteristics. *Proceedings of the IRE*, 1957; 1228–1243.

18. McIntosh KR, Altermatt PP, Heiser G. Depletion-region recombination in silicon solar cells: when does $m_{DR} = 2$?. *Proceedings of the 16th European Photovoltaic Solar Energy Conference*, 2000; 251–254.

19. Green MA. *Solar Cells: Operating Principles, Technology and System Applications*. Prentice-Hall: Englewood Cliffs (NJ, USA), 1982; 96.

20. Araújo GL, Cuevas A, Ruiz JM. The effect of distributed series resistance on the dark and illuminated current-voltage characteristics of solar cells. *IEEE Transactions on Electron Devices* 1986; **33**(3): 391–401.

21. Bowden S, Rohatgi A. Rapid and accurate determination of series resistance and fill factor losses in industrial silicon solar cells. *Proceedings of the 17th European Photovoltaic Solar Energy Conference*, 2001; 1802–1805.

22. Schroder DK, Meier DL. Solar cell contact resistance—a review. *IEEE Transactions on Electron Devices* 1984; **31**(5): 637–647.

23. Ballif C, Huljic DM, Willeke G, Hessler-Wyser A. Silver thick-film contacts on highly doped *n*-type silicon emitters: structural and electronic properties of the interface. *Applied Physics Letters* 2003; **82**(12): 1878–1880.

24. Reeves GK, Harrison HB. Obtaining the specific contact resistance from transmission line model measurements. *IEEE Electron Device Letters* 1982; **3**(5): 111–113.

25. Berger HH. Contact resistance and contact resistivity. *Journal of the Electrochemical Society* 1972; **119**(4): 507–514.

26. Burgers AR, Eikelboom JA, Schönecker A, Sinke WC. Improved treatment of the strongly varying slope in fitting solar cell *I–V* curves. *Proceedings of the 25th IEEE Photovoltaic Specialists Conference*, 1996; 569–572.

27. Sinton RA. Possibilities for process-control monitoring of electronic material properties during solar cell manufacture. *Proceedings of the 9th NREL Workshop on Crystalline Silicon Solar Cell Materials and Processes*, 1999; 67–73.

28. Hoornstra J, van der Heide ASH, Bultman JH, Weeber AW. Simple, detailed and fast firing furnace temperature profiling for improved efficiency. *Proceedings of the Conference PV in Europe—from PV Technology to Energy Solutions*, 2002; 276–279.